Quantum Effects in the Threshold Photoionization and Energetics of the Benzene−H_2O and Benzene−D_2O Complexes: Experiment and Simulation

Alexa Courty, Michel Mons,* Iliana Dimicoli, François Piuzzi, Marie-Pierre Gaigeot, Valérie Brenner, Patrick de Pujo, and Philippe Millié

Service des Photons, Atomes et Molécules, DRECAM, Commissariat à l'Energie Atomique, Centre d'Etudes de Saclay, Bât. 522, 91191 Gif-sur-Yvette Cedex, France

Received: January 13, 1998; In Final Form: May 15, 1998

The present study combines both experiment and molecular dynamics simulations in order to document the ionization behavior of the $C_6H_6-H_2O$ and $C_6H_6-D_2O$ complexes close to the ionization threshold, in particular its nonadiabatic character. Using the two-color two-photon resonant ionization laser technique, the ionization thresholds of these species have been measured together with the threshold for dissociative ionization. A binding energy has been deduced for the neutral species: $D_0(C_6H_6-H_2O) = 106 \pm 4$ meV and $D_0(C_6H_6-D_2O) = 116 \pm 5$ meV, which significantly increases the precision compared to literature. Using a semiempirical potential model, the minimum energy structures of the neutral and ionic species have been determined, and the potential energy surfaces have been analyzed using a two-dimensional approach. As a result, the formation of a stable $C_6H_6^+-H_2O$ complex close to the threshold is found to be controlled by a pure quantum effect and is ascribed to the classically forbidden region of the neutral ground state wave function for the intermolecular vibrational motion. Using classical molecular dynamics simulations in order to sample this region, it has been shown that the neutral conformations involved in the production of stable ions at the ionization threshold exhibit a strong geometry change compared to the neutral equilibrium conformation; i.e., the water molecule is strongly shifted off the benzene C_6 axis and is also flipped over backward the benzene ring. The difference in the ionization energy of the $C_6H_6-H_2O$ and $C_6H_6-D_2O$ complexes, which cannot be explained by the difference in the neutral binding energies alone, supports this result.

1. Introduction

For a long time, ionization of hydrogen-bonded complexes has been recognized as a specific process, due to the geometry change between neutral and ionic.[1−3] In particular, after the pioneering work of Ito and co-workers showing the slowly increasing ionization curve of these complexes,[2] Müller-Dethlefs and co-workers have reported the 1 cm^{-1} resolution two-color ZEKE spectra of the complexes of phenol with several proton acceptors.[3] These ZEKE spectra, which yield the density of vibrational states reached in the ion, have well illustrated the gradual excitation of both intra- and intermolecular vibrational modes when the photon energy is increased. The question of subsequent fragmentation in the complex ion was nevertheless not addressed by these authors.

More recently, the ionization of another type of system, a π-type hydrogen-bonded complex like benzene−water, was shown to produce an efficient ionic dissociation.[4−7] Fragmentation efficiencies as high as 90% were reported in the one-color resonant two-photon ionization (R2PI) of several π-type hydrogen-bonded complexes, like those of benzene with water or hydrogen chloride.[4]

Such a behavior, very different from what is observed in typical hydrogen-bonded complexes, can be easily understood using a simplistic interaction model. Thus, for example, in the benzene−water complex, as revealed by experiments[2−9] or theoretical calculations,[10−20] the water molecule is on one side of the benzene (Bz) molecule, with one (or both) hydrogen atom(s) facing the π-cloud of the Bz molecule. When the complex is photoionized, the repulsive electrostatic interaction of the charged Bz with the permanent dipole of water, which amounts to ∼10 kcal/mol, is high enough to overcome the attractive interactions, namely dispersion and polarization interactions.

With this in mind, it may seem surprising that it is possible to form stable ionic complexes[4−6] and even to measure the photoionization threshold of the $Bz-H_2O$ complex,[21] although the signal intensity appears to be rather small in these photoionization studies. In the synchrotron radiation experiment done by Cheng et al.,[21] the fragmentation threshold of Bz^+-H_2O into $Bz^+ + H_2O$ has also been carried out, which has allowed the authors to derive an experimental binding energy for the Bz−water complex. The modest precision obtained (±12 meV) in this experiment as well as the lack of control of the jet population suggested us to carry out the same type of measurement using an alternative ionization technique: two-color resonant two-photon ionization (2C−R2PI), taking advantage of its high ionization efficiency and its spectral selectivity, offered by the $S_1 \leftarrow S_0$ step. Besides the better sensitivity expected compared to the synchrotron radiation experiment, this technique allows us to measure binding energies and photoionization thresholds of both deuterated and undeuterated neutral species. These binding energies can be compared to the results of a very recent theoretical study of these species by Gregory and Clary.[20]

The aim of the present work is to document the ionization behavior of the $Bz-H_2O$ complex, from the ionization threshold up to the fragmentation limit and to measure the binding energy in the neutral species in a two-color R2PI experiment. In

S1089-5639(98)00761-0 CCC: $15.00
Published on Web 07/23/1998

particular, the effect of deuteration upon the photoionization threshold and the binding energy has been experimentally studied. Alternatively, a theoretical investigation, including intermolecular potential modeling, analysis of the potential energy surface, and molecular dynamics exploration, has also been carried out. In particular, this latter microscopic approach allows us to shed some light on the photoionization process and more specifically to assess which neutral conformations are responsible for energetically stable ionic Bz^+-H_2O complexes.

2. Methodology

2.1. Experiment. The experimental setup, already described elsewhere,[22] combines a supersonic beam, dye lasers, and a reflectron-type TOF mass spectrometer.

The neutral benzene−water complexes are formed in a supersonic expansion of a gas mixture containing the room-temperature vapor pressure of benzene and water (or deuterated water) in helium. The pulsed expansion is generated by a commercial pulsed valve (General Valve) of 0.4 mm diameter nozzle operating at a typical frequency of 15 Hz. The jet is skimmed before entering the mass spectrometer chamber (pressure less than 10^{-6} Torr during operation) parallel to the spectrometer axis. The complexes are excited and ionized by the beam of two dye lasers (Lambda Physik FL 3000 and 2002) pumped by the same excimer laser (Lambda Physik EMG 201). The outputs of the two frequency-doubled dye lasers are conveniently optically delayed in order to cross simultaneously the pulsed molecular beam in the interaction chamber of the mass spectrometer. The ions formed are extracted, accelerated in the spectrometer source, and deflected from the jet axis in order to separate them from the neutral beam and to send them to the electrostatic mirror. After reflection, and drift in a second field-free region, complex ions are detected in a microchannel plate device. The signal is then processed either by a gated boxcar averager or a numeric (LeCroy 9350) oscilloscope.

The photoionization efficiency curves of both the Bz−H_2O and the Bz−D_2O complex have been recorded using the 2C−R2PI technique, taking advantage of its species and state selectivity: the first laser (excitation) is tuned on the $S_1 \leftarrow S_0$ 6_0^1 transition of Bz−H_2O or Bz−D_2O and its intensity is kept low enough in order to minimize the one-color two-photon signal; the second laser scans the ionization threshold region of both the benzene molecule and its complex with water. The photoionization efficiency curve is recorded by processing the mass-selected ion signal in a gated boxcar averager. The ionization energy values given in the present work include correction for electric field ionization ($\Delta(IP) = -kE^{1/2}$ cm^{-1} and $k = 6$).[23]

The first fragmentation pathway of Bz^+-H_2O into $Bz^+ + H_2O$ and of Bz^+-D_2O into $Bz^+ + D_2O$ has been investigated using time-of-flight mass spectrometry. The mass spectra are used to determine ion intensities for both the parent and the daughter ions as a function of the photon energy of the ionization laser, the frequency of the excitation laser being fixed. Some contribution to the ion signal (essentially in the Bz^+ mass channel) was produced from the one-color two-photon ionization process due to the excitation laser. This contribution was measured and subtracted from the two-color measurement. Although the mass spectrometer is operating in the reflectron mode, the mass loss corresponding to the $Bz^+ + H_2O$ fragmentation is nevertheless too large to allow the reflectron to detect the daughter ions due to metastable decay at their true mass. Consequently, the effective time window for fragmentation in the experiment corresponds to ion lifetimes of less than 1 μs. The corresponding kinetic shift is nevertheless expected to remain small, due to the small number (6) of degrees of freedom of the complex. This point will be discussed later.

2.2. Modeling. *2.2.1. Intermolecular Bz−H_2O Potential.* The present calculations are based on a semiempirical intermolecular potential initially proposed by Claverie[24−26] and developed in our group.[27,28] The intermolecular energy is composed of an electrostatic term, a polarization term, and a dispersion−repulsion term. A great effort is realized to calculate very accurately the electrostatic potential energy and the polarization energy. To achieve this, we calculate a multipolar multicentric representation of the electronic and nuclear charge distribution of each molecule of the system. This multipolar multicentric representation is derived from the wave function obtained via an ab initio calculation in which extended atomic basis sets (at least double-ζ) including polarization orbitals must be introduced.[27,28] Moreover, the electronic intramolecular correlation must be taken into account (at least by a second-order Møller−Plesset treatment). In this multipolar multicentric representation, the centers are the atoms and the barycenters of the chemical bonds, and the multipoles are composed of one charge, one dipole, and one quadrupole.[29] Detailed information concerning the determination of the multipolar multicentric representation of the benzene molecule and of the water molecule can be found in ref 30. A specific treatment has been applied for the calculation of the multipolar representation of the benzene cation. We know that in the ground state of the benzene molecule the two energetically highest molecular orbitals (which are doubly occupied) of the benzene molecule are degenerated (π cloud system). In this context, two degenerate states are obtained for the benzene cation in its D_{6h} geometry. Removal of this degeneracy is achieved when a water molecule approaches the cation, thus leading to two different electronic states of the Bz^+-H_2O cluster, each one of different energy. If we neglect, in a first approximation, the coupling between these states induced by the water molecule, the state of the cation that we consider is the one of least energy. We have thus calculated the different multipolar multicentric distributions of the benzene cation, and for each Bz^+-H_2O conformation only the one with the least potential energy is retained.

With this model, the electrostatic interaction energy is the sum of two-body multipole−multipole interactions (from charge−charge interactions to quadrupole−quadrupole interactions). The polarization energy is a *n*-body term which is the sum of the polarization energy of each molecule due to the resultant field created by the multipoles of all the other molecules. In this calculation, the polarizability of each center is derived from experimental molecular polarizabilities. The dispersion−repulsion energy is a sum of atom−atom interactions: the dispersion interaction involves terms up to (C_{10}/r^{10}),[26] and the repulsion energy takes into account the variation of the electronic population of each atom when going from the isolated atom to the same atom in the molecular chemical environment.[28]

In our calculations the Jahn−Teller effect for the benzene cation has not been explicitly taken into account, since recent investigations have shown that the cation should be viewed in D_{6h} symmetry.[31]

2.2.2. Molecular Dynamics Exploration of the Bz−H_2O Potential Energy Surface. We explored the potential energy surface of the Bz−H_2O neutral cluster in order to assess which conformations generate energetically stable ionic Bz^+-H_2O clusters, with a special attention to the photoionization threshold. To this end, we performed classical molecular dynamics simulations. The conditions of the dynamics simulations that

are applied in this study are the same as described in our previous paper.[32] Forces and torques acting on each molecule of the van der Waals Bz−H_2O cluster derive from the intermolecular potential energy described above.

To achieve our goal, we have applied the following process. We explored the Bz−H_2O potential energy surface at a fixed total energy E (microcanonical ensemble). We performed several different molecular dynamics simulations of 300 ps duration each, at the same total energy E, each one differing from the others by the initial cluster conformation (in terms of positions, orientations, and velocities). The integration time step δt was 0.4 fs which gave a conservation of the total energy of the system with a low dispersion value of 10^{-4} over the duration of the simulations. During the simulations, the Bz−H_2O conformations were stored at regular intervals (50 $\delta t = 20$ fs), and for each one we simulated a vertical ionization: the electronic representation of the benzene molecule is changed from Bz to Bz^+ keeping the neutral cluster conformation. Only neutral conformations that lead to ionic potential energies below the dissociation limit are used further in the analysis. This point will be justified later.

3. Experimental Results

3.1. Photoionization Thresholds. Photoionization efficiency spectra of Bz−H_2O and Bz−D_2O have been recorded using the two-color experiment according to the procedure described below. Each species was selectively excited by a first laser to its respective 6^1S_1 state.[4,6,7] The UV spectroscopic shifts of the clusters have been reported in detail by Zwier and coworkers.[7] The transition band contour presents a doublet that has been assigned to two different levels ($m = 0, 1$) of the internal rotation of the H_2O (D_2O) molecule in the complex,[7] which enables us to excite selectively the two subspecies. In the present experiment, photoionization curves of Bz−H_2O and of Bz−D_2O have been recorded with the first laser tuned on the transition from the $m = 0$ ground state.

The photoionization curve of the Bz−H_2O complex (Figure 1a) is found to be noisy, according to the very weak intensity of the $(Bz-H_2O)^+$ signal in this region. The curve increases significantly from a two-photon energy of 9.186 ± 0.007 eV; this onset has been taken at the intercept of the curve slope and the plateau observed below. It should be noticed that, although being very weak, the signal on the plateau is not zero and a detailed observation shows that the intensity vanishes far below the above onset at 9.116 ± 0.007 eV.

A very similar photoionization spectrum is also obtained for Bz−D_2O (Figure 2). One observes also a very weak plateau followed by a significant onset (Table 1). However, the features of the photoionization spectrum (plateau and onset) of Bz−D_2O appear blue-shifted by ∼22 meV relative to those of the Bz−H_2O spectrum.

These results can be compared to the photoionization curve of the Bz−H_2O complex obtained from the one-photon photoionization experiment using synchrotron radiation.[21] These authors report a unique threshold located at 9.170 ± 0.014 eV, which seems to correspond fairly to the major onset observed in the present experiment. However, below this limit, the ion signal level is very low (similar to the noise level) and no clear evidence for the presence of a plateau can be found in their spectrum.

The main characteristics of the photoionization curve of Bz−H_2O and Bz−D_2O is the slow rise of the ion current, which is spread over more than 0.3 eV. This shape is very different from that of the benzene molecule (Figure 1b) or its complexes with rare gases, like argon for example, which is characterized by a succession of steep ionization thresholds, corresponding to the successive excitation of vibrational levels in the Bz^+ cation.[21,33−35]

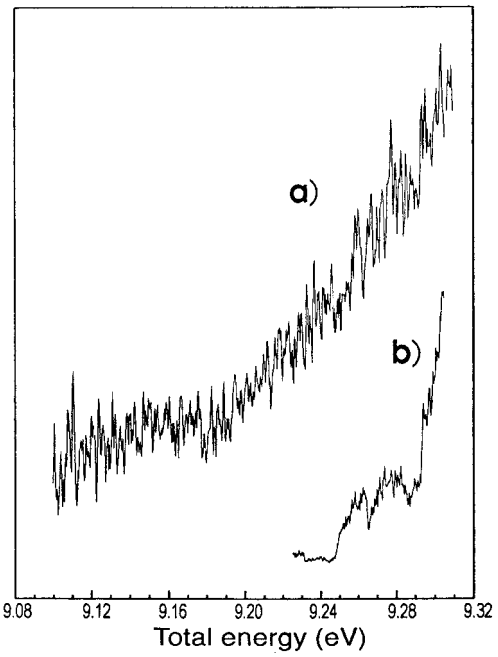

Figure 1. Two-photon photoionization efficiency curves of (a) the benzene−water complex and (b) the benzene monomer pumped in their 6^1S_1 level. The curves are normalized relative to the intensity of the ionization laser and the scaling of the signal intensities is arbitrary. The energies given are corrected for the electric field effect.

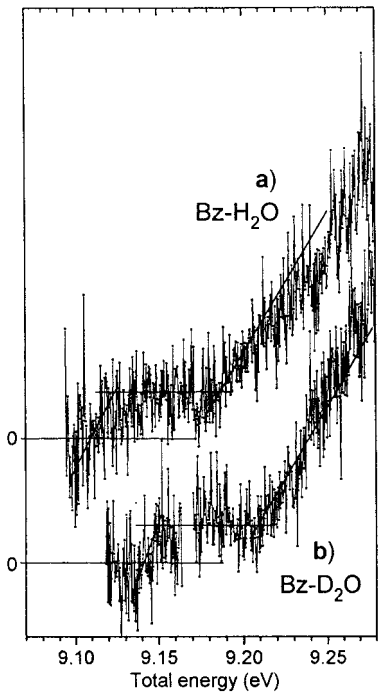

Figure 2. Comparison of the two-photon photoionization efficiency curves of the Bz−H_2O (a) and Bz−D_2O complexes (b). The curves are normalized relative to the intensity of the ionization laser and the energies given are corrected for electric field effect.

Other complexes of benzene, namely Bz_2[36−39] and Bz−HCl,[40] have already been found to exhibit a photoionization curve, similar in some respects to those of Bz−H_2O and Bz−D_2O, in particular characterized by a slow rise of the photoionization current at onset. These photoionization spectra have been interpreted as the signature of a large geometry change between

TABLE 1: Experimental Photoionization Thresholds, Appearance Potentials (AP) of the Fragmentation Process ($(Bz-H_2O)^+ \rightarrow Bz^+ + H_2O$), and Binding Energies (D_0) of the Neutral Species Measured in the Present Work, Compared with Those Found in the Literature[a]

species	photoionization threshold (eV)	AP (eV)	D_0
$Bz-H_2O$			
this work	9.186 ± 0.007	9.354 ± 0.006	2.44 ± 0.09 kcal/mol; 106 ± 4 meV
ref 21	9.170 ± 0.014		2.25 ± 0.28 kcal/mol
ref 7			1.63−2.78 kcal/mol
$Bz-D_2O$			
this work	9.208 ± 0.007	9.364 ± 0.006	2.67 ± 0.11 kcal/mol; 116 ± 5 meV
Bz_2			
this work		9.320 ± 0.007	1.66 ± 0.16 kcal/mol; 72 ± 7 meV
ref 42	8.65 ± 0.01		70 ± 10 meV

[a] The AP and photoionization threshold values given have been corrected for the electric field ionization effect (see text). The precision on these values takes into account the approximate wavelength calibration of the ionization laser. Precision on the D_0 values, which are obtained by difference, is much better.

the neutral and the ionic complex, which forbids the adiabatic ionization.[36,38] A similar explanation seems also to hold for the benzene−water complex. In such a case the Franck−Condon principle forbids the transition from the neutral ground state complex to the ion ground state. Ionization occurs only when the photon energy is high enough to reach the high-lying excited vibrational intermolecular states of the ion, which enables the ion complex to explore conformations similar to those of the neutral ground state.

Thus the major photoionization onset observed allows us to derive a reliable upper limit of the ionization potential (IP = 9.186 ± 0.007 eV). Unfortunately, the beginning of the plateau (Figure 2) cannot be used to propose an improved upper limit. Indeed the weakness of this structure suggests that it might be due to alternative processes: (i) the ionization of van der Waals (vdW) vibrationally excited complexes due to the spectral overlap of the main transition with a hot band. In such a case, the vdW vibrational excitation would favor ionization closer to the ionic well bottom, (ii) the occurrence of an intracluster vibrational redistribution (IVR) in the S_1 state of the benzene−water complex before ionization with the second color takes place. Again the vdW vibrational excitation would lower the ionization threshold. In this case, however, the threshold measured would correspond to an improvement of the upper limit. Unfortunately, from the present experiment, it was not possible to make the difference between the two processes; in particular, two-color experiments with a time delay between lasers could not be carried out with the present setup.

3.2. Appearance Potentials. The smooth onset of the photoionization curve of the $Bz-H_2O$ complex suggests that ionization proceeds according to a broad Franck−Condon zone, spread over more than 0.3 eV above the ionization onset. The large fragmentation ratio (85%) of Bz^+-H_2O that we measure in a one-color ionization experiment (two-photon energy of 9.586 eV) suggests that the ionization should still be possible above 9.25 eV and that in this case it leads to the ionic fragmentation.

Precise investigation of the fragmentation pathway of Bz^+-H_2O and Bz^+-D_2O has thus been carried out in the 9.20−9.40 eV energy range. However, this study is complicated by the presence of the dimer Bz_2^+ in the mass spectrum, which also leads to Bz^+ fragments. Indeed, in a supersonic jet, a great variety of neutral clusters with different sizes are generally formed, and the selectivity of the laser excitation process is not always as large as possible due to an eventual overlap of the $S_1 \leftarrow S_0$ transitions of these species. Under suitable expansion conditions (noble gas pressure, opening time of the valve, delay valve/laser), one has reduced the contribution of Bz_2^+, but not sufficiently to be negligible. Nevertheless, the appearance potential (AP) for the dissociation of Bz_2^+ in Bz^+ has been measured in the present experiment and is found to be equal to 9.320 ± 0.007 eV, leading to a dissociation energy (D_0) of the neutral dimer (Bz_2) of 72 ± 7 meV, according to the relation

$$D_0(Bz_2) = AP(Bz_2^+ \rightarrow Bz^+) - IP(Bz^+) \quad (1)$$

This D_0 value is closed to the value given by Neusser and co-workers (see Table 1), who studied the metastable ions and thus had a larger time window than in the present experiment.[39] The comparison with the experiment of Neusser and co-workers[39] permits thus to validate our results and to ensure that the kinetic shift in our measurement should be negligible. In order to get rid of the benzene dimer contribution, the Bz^+ signal from the Bz_2^+ as a function of total energy has been measured for the excitation of Bz_2 alone and then this undesired signal, suitably scaled, has been subtracted from the Bz^+ production curve following excitation of $Bz-H_2O$.

The production curves of the parents (Bz^+-H_2O and Bz^+-D_2O) and the corresponding fragments Bz^+ as a function of the two-photon energy are shown respectively in Figure 3a and b. In the 9.30−9.35 eV energy range, the increase observed in the parent intensity can be considered as following the slope of the photoionization curve of Figure 2. Then the parent signal is found to saturate at about 9.36 eV. Within the same energy range, the Bz^+ fragment begins to appear and its intensity increases dramatically: 75 meV above the appearance potential of the fragment ion, its intensity is already the same as that of the parent ion. This observation confirms that this energy region still belongs to the main part of the Franck−Condon zone. In other words, there is still a large density of ionic inter- and intramolecular states accessible in this energy range, even if, lying above the AP, these ionic vibrational levels are dissociative and lead to the Bz^+ fragment.

The $AP(Bz^+-H_2O \rightarrow Bz^+)$ and $AP(Bz^+-D_2O \rightarrow Bz^+)$ values have been taken at the intercept of the baseline and the rise of the Bz^+ production curves. The values reported in Table 1 are averaged over several Bz^+ production curves obtained for Bz^+-H_2O and Bz^+-D_2O. The D_0 values have been deduced from the experimental AP value according to the relationship:

$$D_0(Bz-H_2O) = AP(Bz^+-H_2O \rightarrow Bz^+) - IP(Bz^+) \quad (2)$$

which yields D_0 = 106 ± 4 meV for $Bz-H_2O$ and 116 ± 5 meV for $Bz-D_2O$.

The D_0 value obtained for $Bz-H_2O$ compares well with that measured by Grover and co-workers[21] as well as with the spectroscopic bracketing by Zwier and co-workers[7] (see Table 1).

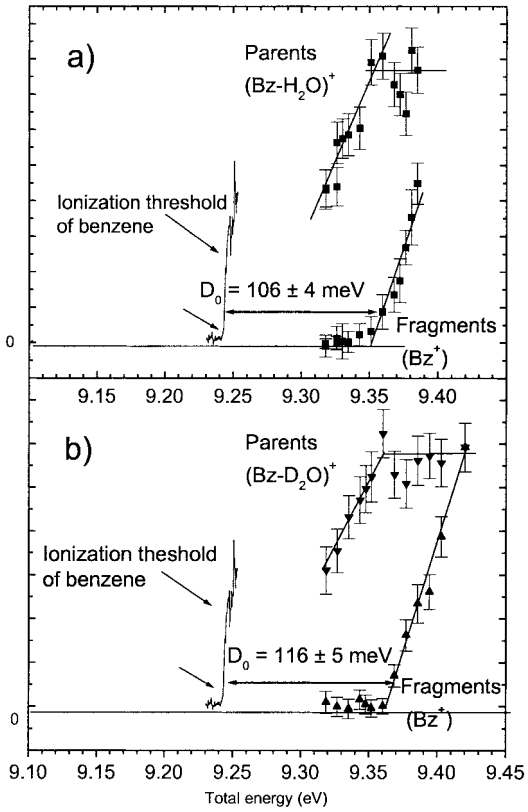

Figure 3. Typical production curves of parent ions (Bz^+-H_2O and Bz^+-D_2O) and of corresponding Bz^+ fragments as a function of the total two-photon energy (eV). The energies given are corrected for electric field effect.

In addition, the present results show that the $Bz-D_2O$ complex is slightly more stable than the $Bz-H_2O$ complex ($\Delta D_0 = 10 \pm 5$ meV $= 0.23 \pm 0.11$ kcal/mol). The D_0 difference between $Bz-H_2O$ and $Bz-D_2O$, which is ascribed to the zero-point energy (ZPE) of the six intermolecular vibrational motion, is in good agreement with the Monte Carlo quantum simulation of the neutral ground-state complexes performed by Gregory and Clary which gives $\Delta D_0 = 0.12-0.19$ kcal/mol, depending upon the interaction potential used.[20]

4. Results of the Molecular Modeling

Experimental studies show that photoionization of the $Bz-H_2O$ complex is mainly followed by ionic fragmentation, in qualitative agreement with the crude model mentioned in the Introduction. Close to the ionization threshold, however, stable ionic Bz^+-H_2O complexes can be formed experimentally. The aim of the present theoretical section is now to understand the reason for the existence of such a minor nondissociative process in the photoionization of the $Bz-H_2O$ complex.

4.1. Equilibrium Structure of the Neutral $Bz-H_2O$ Complex. With our potential, we have found that the water molecule is located just above the benzene ring, in such a way that the oxygen atom stands on the benzene C_6 axis. The distance between the water and the benzene center of masses is 3.16 Å, in reasonable agreement with ab initio calculations,[12,15] although somewhat shorter than the experimental values.[12,14] The planes of both molecules are perpendicular. An illustration of this conformation can be found in Figure 4. As can be seen, the two hydrogen atoms of the water are directed toward the benzene ring in a quasi-equivalent way. Indeed, a small pendulum angle (defined in Figure 5a) is obtained (7°). Thus, the potential energy surface should be of the form of a double well. But, as the energy of the saddle point between the two wells is not significant (10^{-4} kcal/mol relative to the minimum), we can say that the potential energy surface is composed of only one large attraction well.

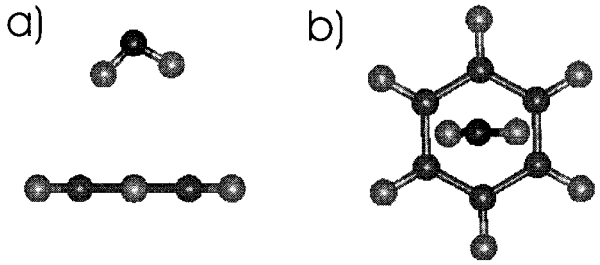

Figure 4. Side (a) and top (b) view of the $Bz-H_2O$ complex equilibrium geometry obtained with the present model.

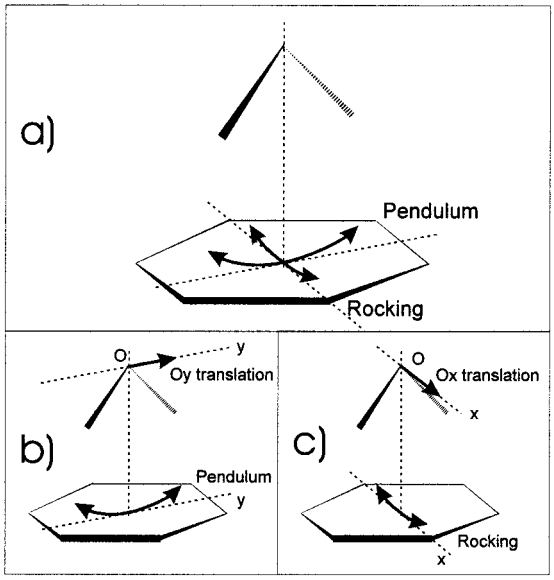

Figure 5. (a) Definition of the *pendulum* (rotation of water in a plane perpendicular to the benzene ring) and *rocking* (back and forth from a plane perpendicular to the benzene ring) motion in the Bz−water complex, starting from a symmetric C_{2v} conformation, close to the neutral equilibrium geometry. (b and c) Representation of the two couples of motions considered in the 2D analysis of the potential energy surface.

Experimental results in an argon matrix[10] and in supersonic expansions[6,7,9,12−14] as well as other theoretical studies using either semiempirical potentials or ab initio methods[15−20] all report only one isomer, in which the water molecule is located above the benzene ring with the oxygen atom on the C_6 benzene axis. However, there is no consensus, either among experimentalists or theoreticians, concerning the number of attraction wells of the potential energy surface: one attraction well if the water hydrogen atoms are equivalently directed toward the benzene ring,[7,10,15−18] a double well if not.[12,14,19] For experimentalists it is very difficult, from spectroscopy alone, to determine the existence of a barrier as well as to decide whether the ground vibrational state is located above the eventual barrier between the two wells or not. A first hint to the absence of significant barrier has nevertheless recently been given by Zwier and co-workers from the fit of the infrared bands of water in the complex.[9] From the theoretical point of view, the ambiguity arises from the coexistence of several interactions, whose variations more or less compensate when the water molecule is rotated. Thus, our potential suggests that the equilibrium geometry results from a subtle compromise between the electrostatic−polarization interactions on the one hand and the

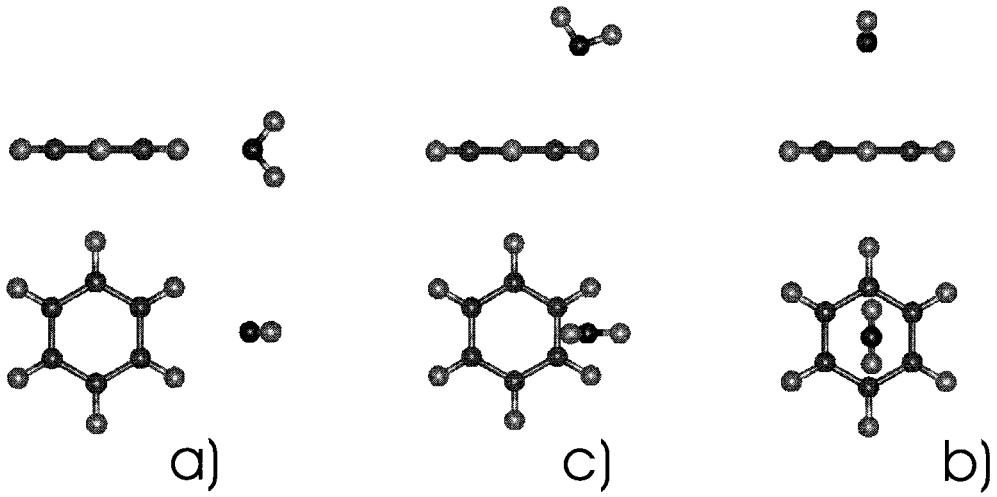

Figure 6. Side and top views of the Bz^+-H_2O equilibrium geometry obtained with the present model for the lowest minimum (a), the second minimum (b) and the saddle point that connects them (c).

dispersion−repulsion interactions on the other hand. Indeed, these two terms vary in the opposite way: the sum of the electrostatic and polarization energies is a weak rising function of the pendulum angle in the interval 0°/40°, whereas the sum of the dispersion and repulsion interactions, which varies in the opposite sense, is maximum for the pendulum angle equal to 0°. This yields an optimum angle of 7° in our equilibrium geometry.

The potential energy of this minimum energy conformation is −3.30 kcal/mol which is consistent with other theoretical investigations that give values in the interval −3.00/−4.00 kcal/mol.[12−20]

4.2. Equilibrium Structure of the Ionic Bz^+-H_2O Complex. With our potential, we find that the Bz^+-H_2O potential energy surface contains two attractive wells. In the more bound equilibrium geometry (Figure 6a), the oxygen atom of the water molecule lies in the benzene plane (4.3 Å from the benzene center of mass), interacting with two hydrogen atoms of the cation, and the hydrogen atoms of the water molecule are symmetrically located aside of the benzene plane. The potential energy of this conformation is −9.22 kcal/mol. The second equilibrium geometry (Figure 6b) corresponds to a water molecule whose oxygen atom stands on the C_6 axis, and with its dipole moment directed opposite to the benzene ring. The intermolecular distance is 3.09 Å and the potential energy is −7.67 kcal/mol.

The saddle point between the two structures (Figure 6c) has been found at an energy of −7.20 kcal/mol and corresponds to a distance of the water center of mass to the benzene C_6 axis of 1.92 Å. This result suggests that the attraction basin of the deepest well is much larger than that of the second isomer.

In contrast to the neutral cluster, there are unfortunately no studies in the literature concerning the ionic cluster to be compared with.

4.3. Two-Dimensional Contour Maps of the $Bz-H_2O$ Complex. In order to give a first insight on the ionization mechanism of the $Bz-H_2O$ complex and to study the neutral configurations able to form energetically stable complex ions, we have first tried to compare the relative positions of both neutral and ionic potential energy surfaces, when the complex conformation is distorted from the minimum geometry. For this purpose, we have carried out 2D contour maps of these surfaces. The choice of the couples of movements considered was suggested by the comparison between neutral and ionic geometries: those in which the water molecule remains above the benzene ring but is flipped over in order to match the orientation of the water molecule in the second isomer of the ion, and those with a water molecule shifted off the C_6 axis of the benzene ring in order to reach the attraction basin of the main ionic isomer. One can note that the reversal of the water molecule can result either from a pendulum movement (in a plane perpendicular to the benzene) or from a rocking movement (back and forth from a plane perpendicular to the benzene), as illustrated in Figure 5a.

From these considerations, we have performed 2D contour maps of the $Bz-H_2O$ neutral and ionic potential energy surfaces (Figures 7 and 8) for the two couples of molecular motions described in Figure 5, b and c. The first couple of motions (Figure 5b) involves the pendulum movement of the water molecule together with the O*y* translation of the water center of mass perpendicularly to the benzene C_6 axis. The second one (Figure 5c) involves the rocking rotation of water and the O*x* translation of the water center of mass from the C_6 axis. These 2D contour maps have been realized with a water center of mass height fixed at the value of the neutral equilibrium geometry.

It can be noted that the initial state considered is the neutral ground state of the complex so that this approach describes not only the one-photon ionization but also the two-photon process. In this latter case, indeed, providing that IVR does not occur as is suggested by the similar ion curves in one- and two-photon experiments, ionization takes place from the lowest intermolecular level of the 6^1S_1 level, which is expected to be very similar to the neutral ground-state level. Two observations support this approximation: (i) S_0 and S_1 binding energies are close one to the other: the spectroscopic vibronic shift of 50 cm^{-1} is small compared to the S_0 binding energy (850 cm^{-1} from the presents results); and (ii) the intermolecular bands observed in the electronic spectroscopy of the benzene−water complex are weak compared to the 6_0^1 transition, which suggests that the two wells exhibit similar shapes.[7]

For the two couples of motions, the 2D contours are very similar and the same comments can be made:

1. One observes a strong potential coupling between the translational and rotational (pendulum or rocking) water motions considered in the neutral state, illustrated by the diagonal orientation of the potential valley in the two couples of motions considered.

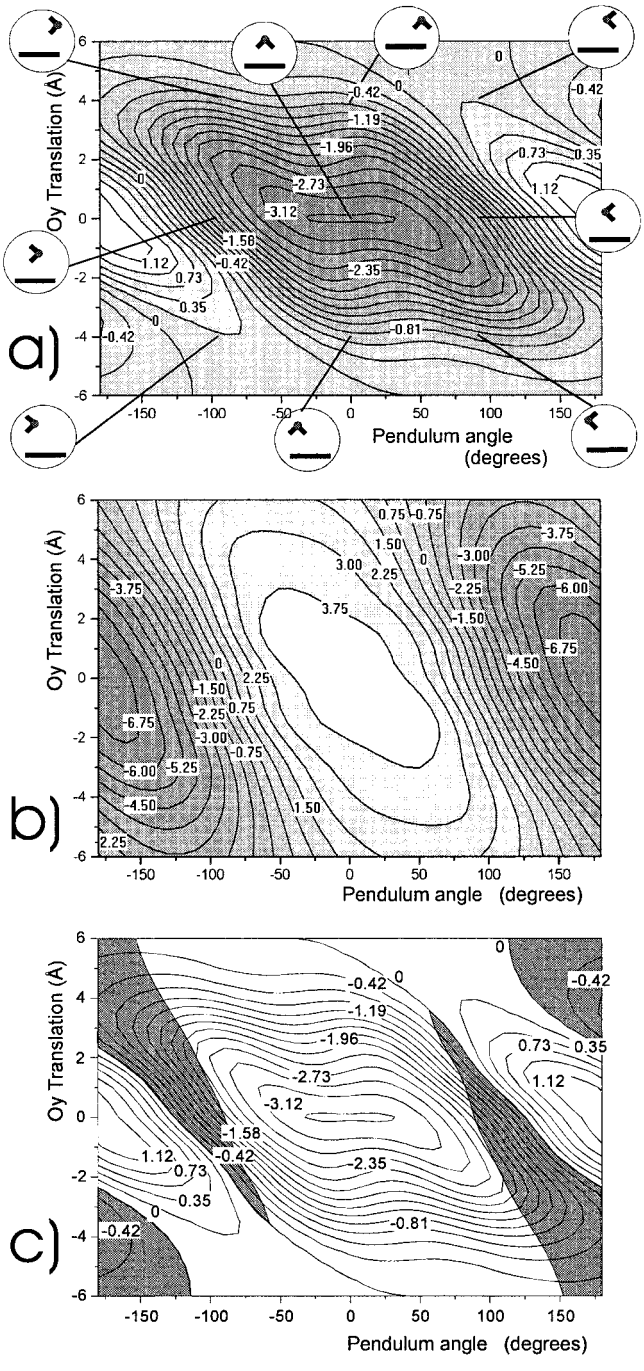

Figure 7. 2D contour maps of the potential energy surface of the benzene−water complex (a) in the neutral ground state, and (b) in the ionic ground state for a couple of motions involving the pendulum movement of the water molecule together with the O*y* translation (Figure 5b) of the water center of mass perpendicular to the benzene C_6 axis. The height of the water center of mass was fixed to the value of the equilibrium geometry. The labels correspond to the potential energy of the isoergic curves, expressed in kcal/mol. In (c) the region of conformations having negative potential energies, in both neutral and ionic ground state, are colored in gray.

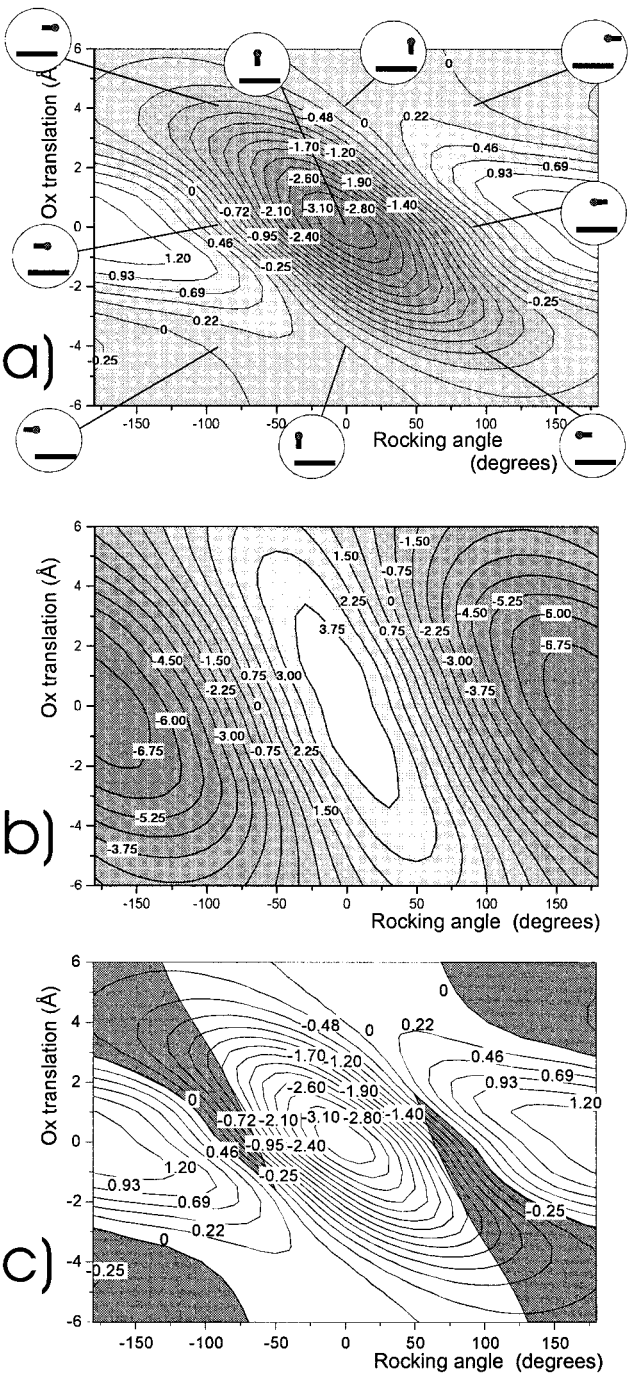

Figure 8. Same legend as Figure 7 for the couple of motions involving the rocking rotation of water and the O*x* translation of the water center of mass from the C_6 axis (Figure 5c).

2. The region around the minimum of the neutral potential energy surface corresponds to a maximum on the ion surface, with positive energies which confirm that the ionization process should be mainly dissociative, in agreement with the large dissociation ratio experimentally measured. This result also suggests that it will not be possible to reach the equilibrium conformations of the ion, i.e., the adiabatic transition between the Bz−H_2O and the Bz^+−H_2O energy surfaces is expected to be forbidden, in agreement with the rough electrostatic model evoked in the Introduction.

The 2D contour maps nevertheless suggest that some neutral conformations can lead to stable ionic conformations. Indeed, such a nondissociative process requires at least that the ionic conformations reached have a negative potential energy. In order to derive more precise information, we have plotted the area corresponding to a negative energy in both the neutral and the ion (Figures 7c and 8c). First, one can note that these overlap regions are rather small and are located far from the neutral minimum. Neutral energies as high as 1 kcal/mol (Figure 7c) and 2 kcal/mol (Figure 8c), expressed relative to the minimum, seem necessary in order to form stable ions and the corresponding conformations correspond to large-amplitude

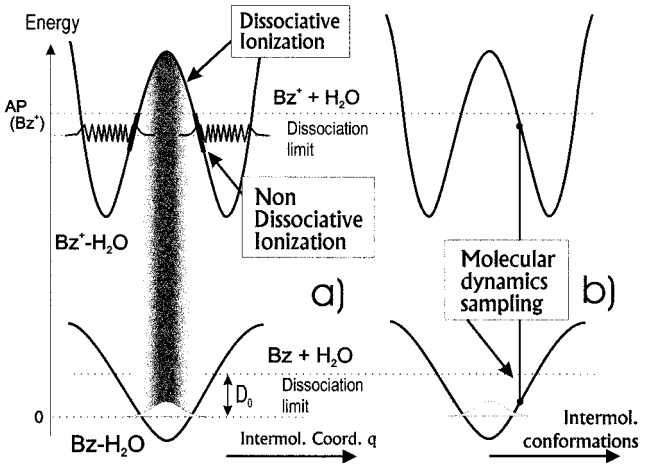

Figure 9. Scheme of the potential energy surfaces of Bz−water pertinent to the analysis of the ionization mechanism, in particular the occurrence of nondissociative ionization. In (a), the intermolecular coordinate *q* chosen for the plot is expected to involve a coordinate leading to the reversal of the water molecule. The vibrational wave function of the neutral state is indicated for the *q* coordinate, together with the oscillating wave function of the high-lying vibrational level reached in the ionic state. In (b) is illustrated the sampling procedure which allows us to evaluate the energy of the conformations reached in the ion as a function of the energy of the neutral conformation.

displacements from the ground state equilibrium geometry. In addition, the corresponding ions are formed in very excited intermolecular vibrational levels close to the dissociation limit.

4.4. Quantum Description of the Ionization of the Benzene−Water Complex. These considerations, namely the role played by the neutral conformations of high energy, raise the question of the energy content of these complexes in the jet. The electronic spectroscopy of these species, in particular the absence of hot bands due to intermolecular modes in the spectra, suggests that the complexes are formed mainly in the vibrational ground state in the jet. Temperatures less than 10 K are currently admitted for complexes of this type in a molecular jet. This suggests that the ionization of the Bz−H_2O complex must be addressed in terms of spatial extension of the quantum ground state for the vibrational intermolecular motion. Since the zero-point energy of the intermolecular vibrational motion should not exceed 1 kcal/mol, according to the work of Gregory and Clary,[20] one must conclude that conformations having ∼1 kcal/mol or more of energy relative to the neutral minimum (Figures 7c and 8c) may be considered as belonging to the tail of the vibrational wave function, located in an area of the space of configurations which is classically forbidden. With this in mind, one can think of the ionization process at threshold as being controlled by pure quantum effects, i.e., the Franck−Condon overlap between the classically forbidden parts of the vibrational ground-state wave function of the neutral and the vibrational wave function of very excited levels of the ion (Figure 9a).

In the present quantum description, we will consider the intermolecular vibrational wave function of the neutral ground state, in which each classical conformation appears with a well-defined quantum probability. Schematically, the higher the potential energy of the conformation, the lower its probability within the wave function. In the present system, if one is interested in the nondissociative process, one has to consider the overlap of the nonclassical tail of the ground state wave function, with very high lying wave functions of the ionic well, as indicated by the 2D contours of Figures 7 and 8. In some respects, this problem resembles closely the absorption process of a molecular ground state to a dissociative electronic state:[41] the high-lying oscillating wave functions of the excited state exhibit a nonvanishing overlap with the bell-shaped vibrational wave function of the ground state essentially because of their behavior at the turning point of the corresponding classical motion on the repulsive inner wall of the potential. For this reason, they are often replaced by a δ function localized at the turning point in order to evaluate the broadness of absorption spectra.[41] The same description (Figure 9a) is expected to hold for the present system.

4.5. Molecular Dynamics Sampling of the Neutral Conformations Responsible for the Nondissociative Ionization of the Benzene−Water Complex. *4.5.1. Sampling Methodology.* In order to investigate more precisely the nondissociative ionization process, in particular to determine the conformations responsible for it, the partial 2D analysis of section 4.3 was complemented by a classical molecular dynamics simulation. This procedure allows us to take into account all the degrees of freedom of the system as well as to compare to role of the two angular motions of the water molecule considered in the 2D analysis.

Indeed, classical molecular dynamics has been considered as a valid approach to sample the neutral conformations belonging to the classically forbidden area of the quantum wave function that is involved in the nondissociative ionization process (Figure 9b). A total energy as high as −0.29 kcal/mol was necessary in order to sample efficiently this set of high-lying conformations. In addition to this, these neutral conformations were considered as ionized through a vertical transition, in agreement with the quantum picture of section 4.4, and the energy of the ionic conformation reached was obtained from the ionic potential in the neutral conformation (Figure 9b).

We first sampled the potential energies of the neutral conformations that lead to nondissociative ionic conformations, i.e., conformations having negative intermolecular energy in the ion. These potential energy values stand between −2.22 and −0.29 kcal/mol (total energy of the simulation). Compared to the equilibrium conformation (energy −3.30 kcal/mol), these conformations are less bound, by at least 1 kcal/mol. The energies of the corresponding ionic species are found to be between −8.68 kcal/mol and zero, which shows that the energy distribution of the ionic complexes is spread over nearly all the accessible ion energy range, i.e., between the minimum energy of the ion (−9.22 kcal/mol) and zero.

The correlation between the potential energy of the initial neutral conformation and the potential energy of the ionic conformation reached is shown in Figure 10, for the neutral conformations that lead to stable ions. From this correlation, several comments can be done:

1. The lowest neutral conformations that give rise to stable ionic complexes leave the ion in very excited states, very close to the dissociation limit.

2. The higher the neutral potential energy, the broader the potential energy range in the ion. In particular, one observes that low-energy conformations in the ion are due to high potential energies of the neutral.

One should, however, note that quantum information lacks in the present results of Figure 10, since we have performed a classical exploration of the neutral potential energy surface. In particular, one can guess that the higher the potential energy of the neutral conformations considered, the lower its quantum probability. In order to overcome this lack of information in the analysis of the neutral conformations responsible for the stable ions, we have taken advantage of the experimental data

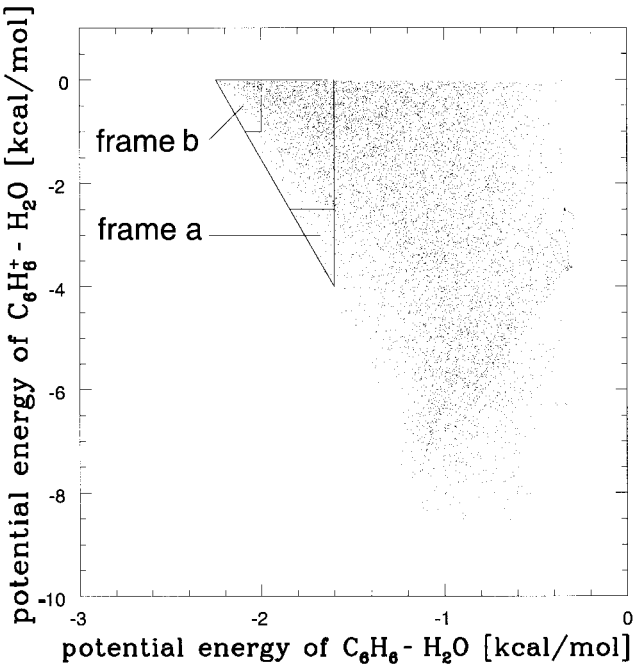

Figure 10. Correlation between the potential energy of the neutral conformations and the potential energy of the corresponding conformation reached in the ion, according to the molecular dynamics sampling of the neutral benzene−water complex. Frame a corresponds to conformations describing the threshold ionization of benzene−water. Frame b corresponds to typical conformations responsible for nondissociative ionization (see text).

available, in particular, the relative positions of the ionization threshold of the complex and the appearance potential of the Bz^+ fragment. This experimental information will allow us to define both neutral and ionic conformations relevant to this discussion.

From the present experimental results (Table 1), we know that the ionization threshold is located ~0.17 eV (3.9 kcal/mol) below the ionic dissociation limit. We can thus deduce that the energy of the bound ion levels formed is spread between −3.9 kcal/mol and zero. This leads to restrict our analysis to the upper part of Figure 10. However, taking into account the quantum weight of these high-energy conformations within the neutral wave function, one can conjecture that only the neutral conformations of low energy will significantly contribute. For this reason we have restricted our analysis to neutral conformations having a potential energy less than −1.6 kcal/mol, which corresponds to the most probable conformations responsible for threshold ionization.

4.5.2. Conformations Responsible for Threshold Ionization. Let us first consider conformations responsible for threshold photoionization. For this purpose, we have considered a set of conformations given by frame a in Figure 10, which corresponds to neutral energies yielding ions close to the ionization threshold. We have thus arbitrarily chosen a set of conformations defined by ionic energies between −3.9 and −2.5 kcal/mol in order to ensure a good statistical sampling and by neutral energies less than −1.6 kcal/mol, which ensures a nonnegligible quantum weight.

The geometry of the corresponding neutral conformations is illustrated (Figure 11) by the correlation between d_{C_6}, the distance of the water center of mass from the benzene C_6 axis, and the orientation of the water molecule relative to benzene (angle ρ between the benzene C_6 axis, oriented from the water to the Bz, and the dipole of the water molecule). In these conformations the water molecule is not only strongly displaced

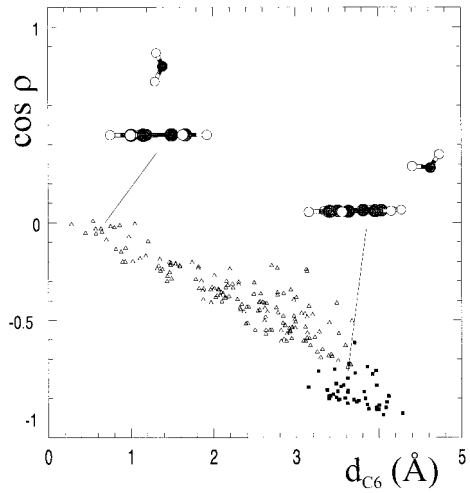

Figure 11. Geometrical characteristics (d_{C_6}: distance of the water molecule center of mass from the Bz C_6 axis, and ρ, angle between the Bz C_6 axis, oriented from the water to the Bz molecule, and the water dipole moment) of the neutral conformations responsible for ionization at threshold (squares corresponding to conformations of frame a in Figure 10) and for typical nondissociative ionization (hollow triangles corresponding to conformations of frame b in Figure 10). A side view of one typical conformation extracted from these two sets is also given.

from the C_6 axis (3−4 Å), which suggests that threshold photoionization forms the ions in the main attraction basin, but is also flipped over relative to the neutral minimum geometry (ρ in the 120−180° range). The water center of mass height value lies between 2.7 and 1.6 Å, which signifies that the water molecule is never located in the benzene plane. The low limit of 1.6 Å illustrates the deficiency of a ionization model based on 2D contour maps alone, which have been carried out at a fixed height corresponding to that of the neutral equilibrium geometry.

In addition, the visualization of these conformations shows that the orientation of the water molecular plane corresponds mainly to a pendulum flip over, as illustrated in Figure 11.

The present investigation demonstrates that ionization at threshold should be ascribed to conformations having a strongly displaced and flipped over water molecule, rather than what have been expected from simple electrostatic arguments, i.e., conformations with a partially flipped over but nondisplaced water molecule.

4.5.3. Conformations Responsible for Stable Ionic Complexes. Let us now consider the conformations responsible for the most intense part of the photoionization curve leading to stable ionic complexes, i.e., the region just below the dissociation limit, as seen in Figures 1 and 3. For this purpose, we have arbitrarily chosen a set of conformations defined by ionic energies between −1 kcal/mol and zero, which correspond to ionization close to the dissociation limit, and by neutral energies less than −2 kcal/mol, which ensures a nonnegligible quantum weight (see frame b, Figure 10).

For these conformations, the d_{C_6} distance is now between 0.6 and 3.6 Å and the water center of mass height lies between 3.5 and 1.8 Å. When the water center of mass is close to the C_6 axis, ionization initially takes place in the second attraction basin, whereas when the water center of mass stands far from the C_6 axis, ionization in the main attraction basin is now favored.

The orientation of the water molecule (angle ρ) and the d_{C_6} distance have also been studied (Figure 11). In all these conformations, the water dipole points mainly backward to the

benzene ring ($\rho > 90°$), which means that only flipped over conformations relative to the neutral equilibrium conformation lead to a nondissociative ionization. More precisely, the visualization of these conformations shows that the orientation of the water molecular plane still corresponds essentially to a pendulum flip over (Figure 11), as in the case of threshold ionization.

One can note from Figure 11 that a strong correlation exists between ρ and d_{C_6}: the higher the angle ρ, the larger the displacement of water from the C_6 axis. This correlation can be ascribed to the potential coupling already mentioned from the potential energy surface analysis of section 4.3.

Figure 11 also illustrates that the conformations responsible for threshold photoionization (frame a in Figure 10) correspond to one part of the set of conformations responsible for the ionization just below the dissociation limit (frame b in Figure 10), namely those with large d_{C_6} distances. This suggests that threshold photoionization occurs first at large d_{C_6} distances in the deepest ionic well and then, as the photon energy is increased, one gradually enables neutral conformations close to the equilibrium geometry to reach stable ionic conformations of decreasing energy. Ionization is finally allowed to occur in the second ionic well, which leads to dissociation at still higher photon energies.

5. Concluding Remarks

Energetics of the Neutral and Ionic Benzene−Water Complexes. The present experiment improves significantly the value of the binding energy D_0 for the Bz−H_2O complex and gives in addition the binding energy of the Bz−D_2O complex with the same precision. These data can be used as a confident basis to validate the model interaction potentials of the literature; in particular, it suggests that, among the two models used by Gregory and Clary,[20] the ab initio fitted potential is the best one, in agreement with the conclusions that these authors derived from the comparison with the experimental geometry.

These binding energy values can also be combined with the estimates of the zero-point energy of these complexes proposed by Gregory and Clary from two model interaction potentials to derive an estimate of the well depth D_e common to both Bz−H_2O and Bz−D_2O species. This combination yields $3.08 \leq D_e \leq 3.53$ kcal/mol, taking into account both the experimental error and the ZPE variations due to the potential used in the simulations. This estimate is in fair agreement with the D_e value of 3.30 kcal/mol of our theoretical semiempirical calculation.

The D_0 values found can be compared to those reported for an apparently similar complex: *p*-difluorobenzene−water (PdFB−H_2O). A spectroscopic study by Martrenchard et al. yields a similar dissociation energy for the neutral complex of 121 ± 7 meV.[30] The PdFB−H_2O complex appears thus only slightly more stable than the Bz−H_2O complex ($\Delta D_0 = 14$ meV), although the nature of the vdW bond differs in the two species: water interacts with one of the fluoride atoms in the former case and with the π system with Bz.[30]

The well depth D_e and the structure of the ion have also been investigated theoretically. The main result is the presence of two isomers that differ from the location of the water molecule relative to the benzene cation; the most bound species has its water molecule in the benzene plane in strong interaction with two hydrogen atoms, which corresponds to a very large geometry change compared to the neutral equilibrium conformation. The ionic well depth found ($D_e = 9.22$ kcal/mol) is much larger than the value proposed by Grover and coworkers,[21] who had wrongly considered the ionization threshold measured as the adiabatic ionization potential.

Photoionization Behavior. The nonadiabatic character of the ionization process of these complexes, suggested by the experimental data, in particular the slow rise of the ion current beyond the threshold and the large fragmentation ratios in the one-color experiments, is confirmed by the analysis of the potential energy curves and the molecular dynamics simulation of these complexes. Experimentally, the fact that we cannot access to the adiabatic ionization potential forbids any precise measurement of the dissociation energy of the ionic complex (D_0^+). Only a coarse lower limit of $D_0^+(Bz^+-H_2O) = 168$ meV (3.87 kcal/mol) can be given.

The model that we propose, illustrated by the scheme of Figure 9, highlights the quantum effects involved in the threshold ionization of the Bz−water complex, in particular, the fact that ionization at threshold does not originate from the maximum of the intermolecular vibrational ground state wave function but rather from its tails associated with distorted conformations in which the water molecule is partially flipped over and/or strongly shifted off the benzene C_6 axis.

Effect of Solvent Deuteration on the Energetics. The same model allows us to interpret also the deuteration effects measured in this experiment, in particular the difference in ionization thresholds between Bz−H_2O and Bz−D_2O. The difference measured, $\Delta IP = 22 \pm 5$ meV, significantly overcomes the difference in the ZPE's: $\Delta D_0 = 10 \pm 4$ meV. Since the ΔIP originates a priori from two independent phenomena, (i) the difference in the ZPE and (ii) the difference in the Franck−Condon overlaps between neutral and ion, one has to conclude that this latter effect contributes to the IP difference to ~12 meV. The model proposed allows us to qualitatively understand this phenomenon in the frame of a quantum description of the intermolecular vibrational motion. Indeed, due to the mass effect, the ground state wave function in the deuterated complex will be less extended than that of the light water species and thus conformations responsible for threshold ionization will be less populated in the deuterated species. As a consequence, the same ion signal level will be observed at a slightly higher photon energy. This qualitative picture, which suggests the occurrence of a pure vibrational quantum effect, is qualitatively confirmed by the quantum wave function calculations by Chavagnac and Clary[42] that have shown the lesser extension of the Bz−D_2O wave function along a coordinate corresponding to the flip over of the water molecule, this molecule remaining in the same plane perpendicular to the benzene.

Acknowledgment. The authors gratefully acknowledge D. C. Clary and A. Chavagnac for providing unpublished results about the ground state vibrational wave functions of Bz−H_2O and Bz−D_2O.

References and Notes

(1) Fuke, K.; Kyoshiuchi, H.; Kaya, K.; Achiba, Y.; Sato, K.; Kimura, K. *Chem. Phys. Lett.* **1984**, *108*, 179.

(2) Gonohe, N.; Abe, H.; Mikami, N.; Ito, M. *J. Phys. Chem.* **1985**, *89*, 3642.

(3) Müller-Dethlefs, K.; Dopfer, O.; Wright, T. G. *Chem. Rev.* **1994**, *94*, 1847 and references therein.

(4) Gord, J. R.; Garett, A. W.; Bandy, R. E.; Zwier, T. S. *Chem. Phys. Lett.* **1990**, *171*, 443.

(5) Gotch, A. J.; Zwier, T. S. *J. Chem. Phys.* **1990**, *93*, 6977.

(6) Gord, J. R.; Garett, A. W.; Severance, D. L.; Zwier, T. S. *Chem. Phys. Lett.* **1991**, *178*, 121.

(7) Gotch, A. J.; Zwier, T. S. *J. Chem. Phys.* **1992**, *96*, 3388.

(8) Pribble, R. N.; Zwier, T. S. *Science* **1994**, *265*, 75 and references therein.
(9) Pribble, R. N.; Garett, A. W.; Haber, K.; Zwier, T. S. *J. Chem. Phys.* **1995**, *103*, 531.
(10) Engdahl, A.; Nelander, B. *J. Phys. Chem.* **1985**, *89*, 2860.
(11) Wanna, J.; Menapace, J. A.; Bernstein, E. R. *J. Chem. Phys.* **1986**, *85*, 1795.
(12) Suzuki, S.; Green, P. G.; Bumgarner, R. E.; Dasgupta, S.; Goddard, W. A., III.; Blake, G. A. *Science* **1992**, *257*, 942.
(13) Dasgupta, S.; Smith, K. A.; Goddard, W. A., III *J. Phys. Chem.* **1993**, *97*, 1081.
(14) Gutowsky, H. S.; Emilsson, T.; Arunan, E. *J. Chem. Phys.* **1993**, *99*, 4883.
(15) Linse, P.; Karlström G.; Jönsson, B. *J. Am. Chem. Soc.* **1984**, *106*, 4096 and references therein.
(16) Brédas J. L.; Street, G. B. *J. Chem. Phys.* **1989**, *90*, 7291.
(17) Cheney, B. V.; Schulz, M. W.; Cheney, J.; Richards, W. G. *J. Am. Chem. Soc.* **1988**, *110*, 4195.
(18) Cheney, B. V.; Schulz, M. W. *J. Phys. Chem.* **1990**, *94*, 6228.
(19) Augspurger, J. D.; Dykstra, C. E.; Zwier, T. S. *J. Phys. Chem.* **1992**, *96*, 7252.
(20) Gregory, J. K.; Clary, D. C. *Mol. Phys.* **1996**, *88*, 33.
(21) Cheng, B. M.; Grover, J. R.; Walters, E. A. *Chem. Phys. Lett.* **1995**, *232*, 364.
(22) Guillaume, C.; Le Calvé, J.; Dimicoli, I.; Mons, M. *Z. Phys. D* **1994**, *32*, 157.
(23) Chewter, L. A.; Sander, M.; Müller-Dethlefs, K.; Schlag, E. W. *J. Chem. Phys.* **1987**, *86*, 4737.
(24) Claverie, P. *Intermolecular Interactions: from diatomics to biopolymers*; Wiley: New York, 1978; Chapter 2.
(25) Langlet, J.; Claverie, P.; Boeuvre, F. J. C. *Int. J. Quantum Chem.* **1981**, *19*, 299.
(26) Hess, O.; Caffarel, M.; Caillet, J.; Huiszoon, C.; Claverie, P. In *Proceedings of the 44th international meeting on modeling of molecular structures and properties*; Rivail, J. L., Ed.; Elsevier: Amsterdam, 1990; p 323.
(27) Brenner, V.; Millié, Ph. *Z. Phys. D.* **1994**, *30*, 327.
(28) Millié, Ph.; Brenner, V. *J. Chim. Phys. (Paris)* **1995**, *92*, 428.
(29) Vigné-Maeder, F.; Claverie, P. *J. Chem. Phys.* **1988**, *88*, 4934.
(30) Brenner, V.; Martrenchard-Barra, S.; Millié, Ph.; Dedonder-Lardeux, C.; Jouvet, C.; Solgadi, D. *J. Phys. Chem.* **1995**, *99*, 5848.
(31) Lindner, R.; Müller-Dethlefs, K.; Wedum, E.; Haber, K.; Grant, E. R. *Science* **1996**, *271*, 1698.
(32) Gaigeot, M.-P.; de Pujo, P.; Brenner V.; Millié, Ph. *J. Chem. Phys.* **1997**, *106*, 9155.
(33) Fung, K. H.; Henke, W. E.; Hays, T. R.; Selzle, H. L.; Schlag, E. W. *J. Phys. Chem.* **1981**, *85*, 3560.
(34) Schmidt, M.; Mons, M.; Le Calvé, J. *Chem. Phys. Lett.* **1990**, *177*, 371.
(35) Krause H.; Neusser, H. J. *J. Chem. Phys.* **1993**, *99*, 6278.
(36) Börnsen, K. O.; Selzle, H. L.; Schlag, E. W. *J. Phys. Chem.* **1988**, *92*, 5482.
(37) Grover, J. R.; Walters, E. A.; Baumgärtel, H. *J. Phys. Chem.* **1989**, *93*, 7534.
(38) Selzle, H. L.; Neusser, H. J.; Ernstberger, B.; Krause, H.; Schlag, E. W. *J. Phys. Chem.* **1989**, *93*, 7535.
(39) Ernstberger, B.; Krause, H.; Kiermeier, A.; Neusser, H. J. *J. Chem. Phys.* **1990**, *92*, 5285.
(40) Walters, E. A.; Grover, J. R.; White, M. G.; Hui, E. T. *J. Phys. Chem.* **1985**, *89*, 3814.
(41) Herzberg, G. *Molecular spectra and molecular structure; I. Spectra of diatomic molecules*; Van Nostrand Reinhold Co. Inc.: New York, 1950; p 392.
(42) Clary, D. C.; Chavagnac, A. *Private communication.*